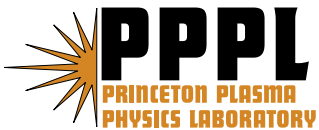# Princeton Plasma Physics Laboratory

Formation of Collisionless High-β Plasmas by Odd-parity Rotating Magnetic Fields

S.A. Cohen, B. Berlinger, C. Brunkhorst, A. Brooks,
N. Ferraro, D.P. Lundberg, A. Roach, and A.H. Glasser

Preprint
(March 2007)

PPPL
PRINCETON PLASMA
PHYSICS LABORATORY

Princeton Plasma Physics Laboratory
Report Disclaimers

Full Legal Disclaimer

Trademark Disclaimer

PPPL Report Availability

Princeton Plasma Physics Laboratory:

Office of Scientific and Technical Information (OSTI):

Related Links:

Formation of collisionless high-β plasmas by odd-parity rotating magnetic fields

S.A. Cohen[a], B. Berlinger[a], C. Brunkhorst[a], A. Brooks[a],
N. Ferraro[a], D.P. Lundberg[a], A. Roach[a], A.H. Glasser[b]

January 14, 2007

Abstract

Odd-parity rotating magnetic fields (RMF_o) applied to mirror-configuration plasmas have produced average electron energies exceeding 200 eV at line-averaged electron densities of $\sim 10^{12}\ cm^{-3}$. These plasmas, sustained for over $10^3\ \tau_{Alfven}$, have low Coulomb collisionality, $\nu_c^* \equiv L/\lambda_C \sim 10^{-3}$, where λ_C is the Coulomb scattering mean-free-path and L is the plasma's characteristic half length. Divertors allow reduction of the electron-neutral collision frequency to values where the RMF_o coupling indicates full penetration of the RMF_o to the major axis.

The field-reversed configuration[1, 2] (FRC) is a high-β (plasma pressure/magnetic-field energy density) plasma confinement concept that possesses many attractive features favoring its development into a practical fusion reactor. To reach this goal, physics research must find viable methods to achieve adequate energy confinement, to maintain plasma stability, to drive plasma current for sustaining the configuration, and to heat the plasma to fusion-relevant temperatures. The rotating magnetic field (RMF) technique, conceived[3] as a method to generate plasma current, also has the potential to heat and stabilize plasma.[4, 5, 6] RMF research should be performed at low ν_c^*, to explore the physics regime relevant to fusion reactors.

Plasma formation by even-parity RMFs (RMF_e), the geometry pioneered in the 1980's in the rotamak series of experiments,[7] has not been successful in producing collisionless FRC plasmas, sustaining only warm electrons, $T_e \leq 50$ eV, in relatively dense and large plasmas, even for heating powers in excess of 2 MW.[8] Some, *e.g.*, ref. [8], attributed the limitation to a radiation barrier, though Bellan showed that the energy loss from RMF_e-heated devices was at a rate consistent with ion-acoustic flow,[9] evidence for open field lines predicted by theoretical work.[10] Six years ago, theoretical analysis demonstrated that low amplitude transverse fields of odd parity would maintain the closure of an FRC's field lines.[11] Soon after, theoretical research showed that fully penetrated odd-parity RMFs (RMF_os) could effectively heat ions and electrons in collisionless FRCs.[4, 5, 12]

Electron energy is a natural measure of confinement quality and heating physics. The experiments described herein measured β and electron density and energy in plasmas generated by RMF_o, testing the hypothesis that this novel symmetry-preserving class of rotating magnetic fields can effectively heat electrons at low ν_c^*. Our novel results include the RMF_o generation of low ν_c^*, high-$\langle\beta\rangle$ plasmas with electron temperatures well above 100 eV, sustained for more than 10^3 τ_{Alfven} and with the RMF_o fully penetrated to the major axis.

Achieving high T_e in a plasma by the application of time-varying fields is difficult if the only scattering process is Coulomb and fundamental resonances are absent. However, the FRC's magnetic field is highly inhomogeneous, allowing for electron scattering by bends in the magnetic field[13] and by crossing a phase-space separatrix.[12] A numerical study[5] of electron dynamics in FRCs with RMF_os at frequencies far below the electron cyclotron frequency showed periodic electron acceleration near and along the O-point null line with energy oscillations, $\Delta W_M \sim |eB_R\omega_R r_s^2|$, where B_R is the RMF_o amplitude, ω_R is the RMF_o angular frequency, e is the electron charge, and r_s is the FRC separatrix radius. A slow secular increase in the average electron energy, to $\Delta W_M/3$, results, due to the aforementioned collisionless scattering. Such scattering events increase plasma resistivity, impacting plasma heating, current drive, and RMF penetration.

Recent modifications to a 40-cm-radius, 3-m-long FRC device allowed RMF_o studies at 1 MW of heating power and showed encouraging results, notably improved stability against the $n = 2$ interchange mode [14] and reduced conduction losses[15]. In the latter experiments, the total temperature (electron *plus* ion) increased from 22 to 32 eV. Plasma impurities and lack of density control were thought to have created a radiation barrier, limiting T_e and RMF_o penetration. Due to Coulomb collisions at this low T_e, the large machine size, moderate density, and frequent electron-neutral collisions in this device's high recycling geometry, the plasma remained in the collisional regime, $\nu_c^* \sim 1$, where heating and transport are dominated by binary collisions rather than field closure and collisionless scattering. Higher T_e, lower neutral pressure, lower plasma density, and smaller device size are paths to a low-ν_c^* reactor-like regime.

Our approach to low ν_c^* employs high-ω_R low-B_R RMF_o, consistent with conditions for RMF current drive and penetration.[16] Density control is critical. The Princeton FRC (PFRC) device, with internal flux conservers and two divertors for reducing recycling, neutral density and plasma density (see Fig. 1), was designed and operated based on these principles. Four 29-cm-long RF-powered RMF_o antennas are placed symmetrically about the PFRC midplane and outside its 10-cm-ID, 81-cm-long multi-port Pyrex vacuum vessel. At each end of the Pyrex vessel are sets of three co-axial magnet coils (A1, B1 and N1 and A2, B2 and N2) which produce a weak (B_0 to 400 G) predominantly axial field at the midplane and a stronger mirror field (B_M to 5000 G) at the centers of coils $N1$ and $N2$. Nested in each ABN coil set is a divertor chamber. Centered inside the Pyrex vessel is a co-axial 33-cm-long array of ten copper rings. These rings, separated from each other by 3-6 cm, function as flux conservers (FCs), to slow radial expansion of the magnetized plasma column. The FC array has a skin time, τ_s, of 3 ms. The inner radii of the FC rings vary from $r_{FC} = 4.15$ cm to 2.75 cm, with smaller IDs further from the Pyrex vessel's midplane. Co-planar with

2

and mounted radially inboard of the 4th and 7th FCs (and elsewhere) are diamagnetic loops (DL). A 170-GHz interferometer views the plasma radially between the 3rd and 4th FCs. X-ray and visible-wavelength spectroscopy diagnostics view the plasma 6.5 and 23 cm from the midplane.

To form plasmas of line-average density $\bar{n}_e = 10^{11-13}$ cm^{-3}, a static mirror-geometry magnetic field is established in the Pyrex vessel by the ABN coils. H_2, D_2 and/or He gas is then flowed through the Pyrex vessel, raising the pressure to 0.4 - 40 mTorr. RF power, P_{RF}, is transmitted to the four antennas through tank circuits and applied in 0.1 to 15-ms-duration pulses at a duty factor of 0.5%. The RF frequency, $f_{RF} \equiv \omega_R/2\pi$, controllable to one part in 10^8, is set close to the resonance of the RMF_o antennas *plus* tank circuits subsystem which has Q in the range $60-160$ at 14 MHz in the absence of plasma. P_{RF} is increased until pulsed plasmas have formed, at which point Q drops by $10-70\%$. The maximum net RF power (forward - reverse, $P_f - P_r$) is $P_{RF} = 11$ kW; up to 7 kW has been coupled to the plasma. f_{RF} may be modulated during a pulse. We typically use square-wave FM, with shifts in frequency as large as 250 kHz. We first describe results without FM.

Figures 2a) and b) show data from a pulse with $B_0 = 55$ G, H_2 fill pressure $P_{H_2} = 1.25$ mTorr, and $f_{RF} = 14.062$ MHz, 70 kHz above the resonant frequency with no plasma, f_v. $\bar{n}_e$, calculated with the assumption that the plasma diameter was 8 cm, quickly rises to 0.5×10^{12} cm^{-3}, maintains that value for 1.8 ms, and then steadily declines, falling to near zero before the RF power is terminated at 3.2 ms. (Higher P_{H_2} results in a longer $\bar{n}_e$ flat-top.) The diamagnetic-loop-measured flux change, Φ_{DL}, was 60 nVs at the initiation of the discharge. In 2 ms Φ_{DL} rose at an increasing rate to 600 nVs, remained there for 0.8 ms, and then began to fall just after $\bar{n}_e$ began its decline. (Φ_{DL} returns to zero at ~ 3 τ_s after the RF power is shut off.) P_{RF} initially rises to 4 kW, then steps to 9.4 kW, remaining there for 1 ms. Over the next 2 ms P_{RF} steadily declines to 4 kW. The RF voltage reflection coefficient, $R_{RF} \equiv \sqrt{P_r/P_f}$, is initially high, 0.6 for $t = 0 - 0.15$ ms, because $f_{RF} \neq f_v$. At $t = 0.15$ ms, R_{RF} drops below 0.1 and remains there until $t = 1.0$ ms. R_{RF} increases through the rest of the pulse. The maximum power coupled to this plasma was 3 kW. Concurrent with the decrease in RF coupling during the time t = 1.0-3.2 ms is a decrease in H_α radiation. The good RF coupling from 0.16 to 1.0 ms is due to f_{RF} being very close to the system (*i.e.*, antennas + tank circuits + plasma) resonant frequency, f_s. Exclusion of the RMF_o from part of the volume occupied by the plasma lowers the inductance of the RMF_o system, raising f_s. Thus, the reason why f_{RF} is initially set above f_v is to improve power coupling when there is poor RMF_o penetration into the plasma. The change in RF coupling after 1.0 ms is caused by a change in f_s due to evolving plasma parameters.

$\bar{n}_e$ and Φ_{DL} were measured at an absorbed power of ~ 6 kW for a range of B_0 values. The maximum achieved $_m\Phi_{DL}$ are plotted in Fig. 3, along with $\langle\beta\rangle$ values, calculated using the method detailed in the next paragraph, based on the equations in [17] for $\langle\beta\rangle > 0.5$ and in [18] for $\langle\beta\rangle < 0.5$. For $\langle\beta\rangle > 0.5$, ref. [17] assumes a separatrix surface inside which the magnetic flux is zero. For $\langle\beta\rangle < 0.5$, no magnetic separatrix is assumed. Note that we have no direct experimental measurements that can unambiguously distinguish between a closed-field-line FRC and a high-β mirror configuration. For $B_0 < 70$ G, reference [17]

indicates that the plasma may be in a field-reversed configuration while for $B_0 > 70$ G it is in a mirror configuration. At the larger B_0 values, $\bar{n}_e$ showed strong periodic fluctuations (50 kHz at $B_0 = 200$ G decreasing to 15 KHz at $B_0 = 400$ G), reaching $\tilde{n}_e/\bar{n}_e \sim 0.5$ at $B_0 = 350$ G.

Analyses of Φ_{DL} and X-ray spectra were performed to extract T_e. The measured Φ_{DL} was compared with that calculated by a numerical model of the electrical current evolution in the plasma, flux conservers, and diamagnetic loops and with experimental calibrations using a pulsed solenoid. The plasma was assumed to have the shape of a Hill's vortex with elongation $\kappa \equiv L/r_s = 5$. Time-dependent simulations of diamagnetic loop signals were made for a range of r_s values and FRC plasma current profiles, generating a graph of $_pB_0$ vs r_s per ampere of FRC current, where $_pB_0$ is the on-axis midplane field with an FRC plasma. This graph was compared with the $_pB_0$ that would result when FRCs of different r_s were formed at an initial bias field of B_0: $_pB_0(r_s) = -B_0 r_{FC}^2/(r_{FC}^2 - r_s^2)$, which assumes perfect flux conservation by the FCs, accurate to better than 15% for times less than 1 ms. The intersection of these two graphs gives r_s and $_pB_0$. (For $B_0 \sim 60$ G, r_s was usually in the range 1.9-3.0 cm and $|_pB_0/B_0| = 1.25 - 2.1$.) Given the measured $\bar{n}_e$ and assuming a uniform density profile, T_e is extracted by use of the Barnes relation[19], $\langle \beta \rangle = 1 - (r_s/r_{FC})^2/2$. (The Barnes relation does not include plasma pressure or radial field beyond the X-point, hence gives a lower limit on $\langle \beta \rangle$.[17]) Typical values were: $\langle \beta \rangle = 0.75 - 0.9$ and $T_e = 100 - 200$ eV, with the lower T_e obtained if n_e was assumed to be zero outside r_s. (This is not considered likely because the gyroradii of both 100-200 eV electrons and 0.4 eV H^+, the latter determined by Doppler broadening measurements of H_α, are ~ 0.5 cm.) These experiments show strong evidence for intense hydrogen recycling caused by radial losses to the flux conservers, especially at lower B_0 and during the $\bar{n}_e$ flat-top.

Si-diode[20] X-ray spectroscopy showed X-rays at energies between 0.6 and 4 keV. One spectrum is shown in Fig. 4, corrected for both the measured detector resolution and a transmission coefficient, from the literature, of the 1-mil Be vacuum window in front of the detector. The spectrum between 900 and 1900 eV, accumulated for $0 < t < 3.75$ ms of 4348 highly reproducible discharges, shows an exponential shape fit by $T_e = 150 \pm 25$ eV.[21] Bremsstrahlung from the PFRC is primarily due to electron collisions with neutral hydrogen[22, 23] because $5 < (n_{H^o} + 2n_{H_2})/n_{H^+} < 500$. From the highest T_e attained, 230 eV at $\bar{n}_e = 1.5 \times 10^{12}$ cm^{-3}, $B_0 = 60$ G and 7 kW absorbed RMF_o power, T_e falls as the power is reduced or B_0 is increased. For $B_0 \geq 130$ G or low n_{H_2}, the X-ray count rate is too low to allow a T_e determination. At $T_e = 100$ eV and $n_e = 10^{12}$ cm^{-3}, the Coulomb collisionality is $\nu_c^* \equiv L/\lambda_C = 10^{-3}$, assuming $L = 16.5$ cm, half the length of the FC array.

The RMF code[5] was used to explore RMF_o "collisionless" electron heating. Using $r_s = 3$ cm, $\kappa = 5$, $f_{RF} = 14$ MHz, $_pB_0 = 120$ G and $B_R = 10$ G, the RMF code does predict average electron energies of 230 eV (see inset Fig. 4), a value very close to $3T_e/2$. The code also shows good single-particle confinement, > 40 μs. However, for initial electron energies near 5 eV, the code shows a cut-off in energy at 700 eV, not the exponential tail seen in the X-ray data. An exponential tail might arise from Coulomb or neutral particle scattering not in the RMF code. (RMF simulations of the initial PFRC mirror configuration show less

4

electron heating and rapid electron loss, in less than $0.4 \mu s$ for $B_R > 3$ G.)

Refinements to the experimental methodology, particularly the use of FM and of divertors, produced higher peak Φ_{DL}, to 5 $\mu V s$, at low B_0, 55 G. The unique FM capability of the PFRC RF system allows in-discharge compensation for changes in f_s caused by evolving plasma characteristics. Quantification of the shift-in-resonance provides non-invasive diagnosis of the RMF_o penetration depth into the plasma column, as now described.

If the RMF_o does not penetrate into the approximately cylindrical volume occupied by the plasma, the inductance of the RMF_o system is lowered and the resonant frequency rises by $\Delta f_p = \alpha \, r_e^2$, where r_e is the effective radius of the cylindrical volume inside which the RMF_o does not penetrate. (By placing metal rods of varying diameters along the PFRC major axis and measuring the shift in resonance, α was determined to be 13.3 kHz/cm^2.) First, without plasma, we scan f_{RF} to measure the system resonant frequency: $f_s = f_v =$ 13.992 MHz in this example, see Fig. 2c). Then, with $P_{H_2} = 1.25$ mTorr, $B_0 = 55$ G and $B_M = 2900$ G, RF power is applied to the antennas in 2-ms-duration pulses. The plasmas formed initially shift f_s away from f_v, as evidenced by an increase in R_{RF}. To increase the power coupling to the plasma during the initial 1 ms of the discharge, f_{RF} is set above f_v, typically to $f_p = f_v + \Delta f_p \sim 14.062$ MHz, which lowers R_{RF} to 0.1, see $t = 0.2 - 1$ ms in Fig. 2b). (The Δf_p required to minimize R_{RF} increases with increasing P_{H_2} and B_0, see Fig. 2c).) Then, the RMF_o pulse length is stretched to 3.2 ms, to allow gas in the Pyrex vessel to be ionized and exhausted into the divertor chambers. From t = 1 to 2.7 ms R_{RF} slowly increases. In a sequence of discharges, f_{RF} at 2.7 ms is shifted differing amounts, $i.e.$, FM, to search for the frequency, $^*f_{RF}$, which gives the lowest R_{RF}, see Fig. 2f), and highest RF-power coupled. Pronounced increases in $\bar{n}_e$ and Φ_{DL}, see Fig. 2d), occur at $^*f_{RF}$. For cases where $^*f_{RF} = f_v$, the RMF_o is deemed to have fully penetrated to the PFRC major axis. H_α spectroscopy and a fast pressure gauge in the Pyrex chamber confirm reduction in neutral gas density, the latter showing $n_{H_2} < 10^{13}$ cm^{-3} in the Pyrex chamber when $^*f_{RF} = f_v$. Timing and sizing the FM, change of fill-gas pressure, and control of RF power have allowed the FM-mediated $\bar{n}_e$ and Φ_{DL} increases to be maintained for > 1 ms.

One other RMF/FRC group[24] has reported full RMF penetration. That, too, was achieved at low neutral pressures. Consideration of elastic electron-neutral scattering[25] and collisional ionization predicts that a neutral $(2n_{H_2} + n_H)$ density below 5×10^{13} cm^{-3} is required for full RMF penetration into the PFRC at $T_e = 100$ eV, using the penetration criterion of Jones and Hugrass[16] with plasma resistivity modified to include electron collisions with neutrals. This density exceeds our result by a factor of 2.5, perhaps indicating the importance of other scattering processes, $e.g.$, Speiser, or corrections needed to the Jones and Hugrass model to account for RMF_o applied to a kinetic (rather than MHD) plasma. Based on the results presented here, Speiser scattering should not prevent RMF penetration into a reactor-scale[4, 5] advanced-fuel-burning FRC.

In summary, relatively low amplitude ($B_R/_pB_0 \sim 0.1$) RMF_os have produced H^+ plasmas with T_e up to 225 eV, $\langle \beta \rangle = 0.75 - 0.9$, and $r_s = 1.9 - 3$ cm at $\bar{n}_e \sim 10^{12}$ cm^{-3}, corresponding to $\nu_c^* \sim 10^{-3}$. No radiation barrier was encountered. The Bremsstrahlung

spectrum from electron-neutral collisions is consistent with a Maxwellian electron energy distribution. Though the average electron energy is consistent with collisionless RMF_o heating in an FRC, the detailed shape of the X-ray spectra is not. Full penetration of the RMF_o to the major axis occurred at molecular hydrogen densities below 10^{13} cm^{-3}.

[a] Princeton Plasma Physics Laboratory, Princeton University, Princeton, NJ
[b] Los Alamos National Laboratory, Los Alamos, NM

References

[1] N.C. Christofilos. *Proc. of the 2nd UN Conf. on Peaceful Uses of Atomic Energy* **32**, *(Geneva)*, page 279, (1958).

[2] M. Tuszewski. *Nucl. Fusion* **28**, page 2033, (1988).

[3] H.A. Blevin and P.C. Thonemann. *Nucl. Fusion Suppl.* **1**, page 55, (1962).

[4] S.A. Cohen and A.H. Glasser. *Phys. Rev. Lett.* **85**, page 5114, (2000).

[5] A.H. Glasser and S.A. Cohen. *Phys. Plasmas* **9**, page 2093, (2002).

[6] S.A. Cohen. *Bull. Am. Phys. Soc.* **44**, page 596, (1999).

[7] I.R. Jones. *Phys. Plasmas* **6**, page 1950, (1999).

[8] A.L. Hoffman, H.Y. Guo, K.E. Miller, and R.D. Milroy. *Phys. Plasmas* **13**, page 012507, (2006).

[9] P.M. Bellan. *Plasma Physics and Controlled Fusion* **31**, page 879, (1989).

[10] W.N. Hugrass and M. Turley. *J. Plasma Physics* **37**, page 1, (1987).

[11] S.A. Cohen and R.D. Milroy. *Phys. Plasmas* **7**, page 2539, (2000).

[12] A.S. Landsman, S.A. Cohen, and A.H. Glasser. *Phys. Rev. Lett.* **96**, page 015002, (2006).

[13] T.W. Speiser. *J. Geophys. Res.* **70**, page 4219, (1965).

[14] H.Y. Guo, A.L. Hoffman, R.D. Milroy, K. E. Miller, and G. R. Votroubek. *Phys. Rev. Lett.* **94**, page 185001, (2005).

[15] H.Y. Guo, A.L. Hoffman, and L.C. Steinhauer. *Phys. Plasmas* **12**, page 062507, (2005).

[16] I.R. Jones and W.N. Hugrass. *J. Plasma Phys.* **26**, page 441, (1981).

[17] W.T. Armstrong, R.K. Linford, J. Lipson, D.A. Platts, and E.G. Sherwood. *Phys. Fluids* **24**, page 2068, (1981).

[18] M.A. Rothman and W.M. Hooke. NTIS PB2007-104979. *Technical Memo-215: Princeton Plasma Physics Laboratory*, (1965).

[19] D.C. Barnes, C.E. Seyler, and D.V. Anderson. *Proc. of the US-Japan Joint Symp. on Compact Toruses and Energetic Particle Injection, (Princeton)*, page 110, (1979).

[20] Amptek Inc. Model xr-100cr. *14 De Angelo Drive, Bedford, MA 01730.*

[21] I.H. Hutchinson. *Principles of Plasma Diagnostics.* Cambridge University Press, New York, 2nd edition, 2002.

[22] Lee Estep and C.A. Quarles. *Physica* **145C**, page 369, (1987).

[23] Young-Dae Jung. *Applied Physics Letters* **86**, page 211504, (2005).

[24] H.R. Zwi, A. Kuthi, A.Y. Wong, and B. Wells. *Phys. Fluids B* **3**, page 126, (1991).

[25] B. van Wingerden, E. Weigold, F.J. de Heer, and K.J. Nygaard. *J. Phys. B: Atom. Molec. Phys.* **10**, page 1345, (1977).
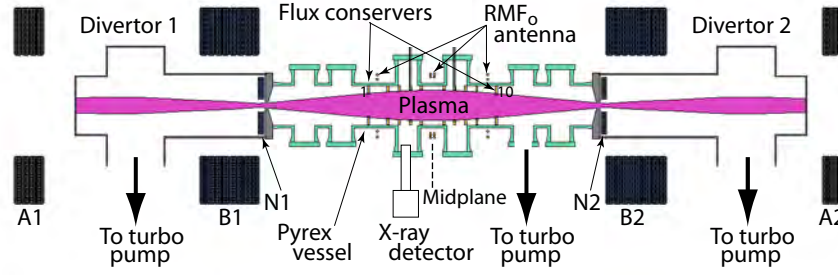
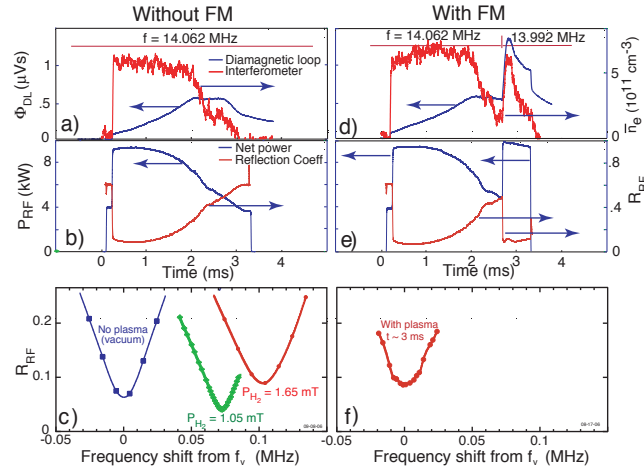Figure 1: PFRC Schematic. Scaled cross-sectional view.

Figure 2: Upper group: Time evolution of Φ_{DL}, $\bar{n}_e$, P_{RF}, and R_{RF} for hydrogen discharges. a) and b) are at fixed frequency, 14.062 MHz; in d) and e) the frequency was shifted (FM) to 13.992 MHz at 2.7 ms during the discharge. Lower group: R_{RF} *vs* RMF_o frequency relative to f_v: c), for three conditions: 1) without plasma; 2) at $t \sim 1$ ms in discharges with $P_{H_2} = 1.05$ mTorr ($B_0 = 55$ G); and 3) with $P_{H_2} = 1.65$ mTorr ($B_0 = 122$ G); f), at $t \sim 3$ ms, *i.e.*, after FM, in discharges with $P_{H_2} = 1.25$ mTorr.
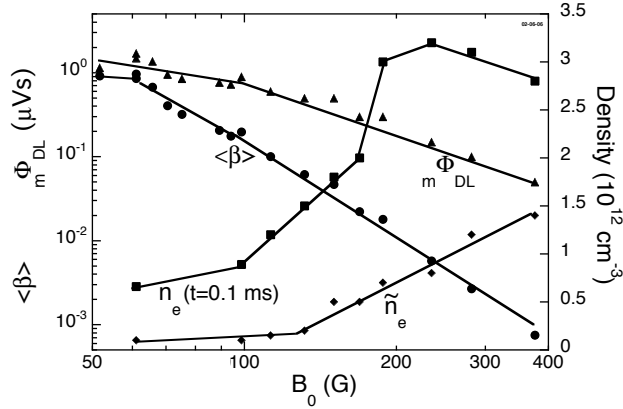
Figure 3: Measured $_m\Phi_{DL}$, $\langle\beta\rangle$, $\bar{n}_e$, and $\tilde{n}_e$, vs B_o. Pulse duration $t = 2$ ms, max $P_{RF} = 9.6$ kW, $f_s = 13.967$ MHz, $P_{H_2} = 1.08$ mTorr, $B_M = 2800 - 5000$ G.
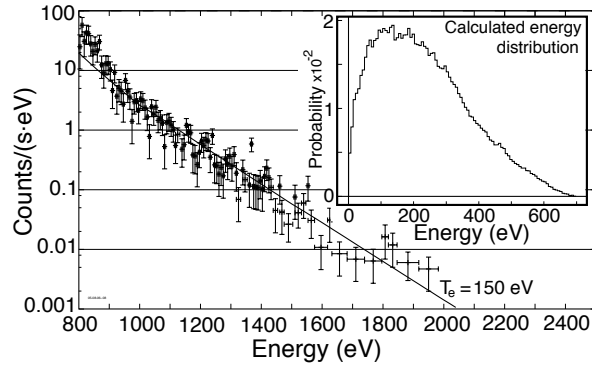

Figure 4: Measured X-ray spectrum: $_mP_{RF} = 9.6$ kW; $_mn_e = 1.6 \times 10^{12}$ cm^{-3}; $_m\Phi_{DL} = 5\mu Vs$; $f_s = 14.000$ MHz (no FM); $P_{H_2} = 1.09$ mTorr; $B_0 = 56$ G; $B_M = 2900$ G, where subscript m means maximum value. The spectrum shape is fit by $T_e = 150$ eV. Inset: Electron energy distribution calculated with the RMF code.

The Princeton Plasma Physics Laboratory is operated
by Princeton University under contract
with the U.S. Department of Energy.

Information Services
Princeton Plasma Physics Laboratory
P.O. Box 451
Princeton, NJ 08543

Phone: 609-243-2750
Fax: 609-243-2751
e-mail: pppl_info@pppl.gov
Internet Address: http://www.pppl.gov